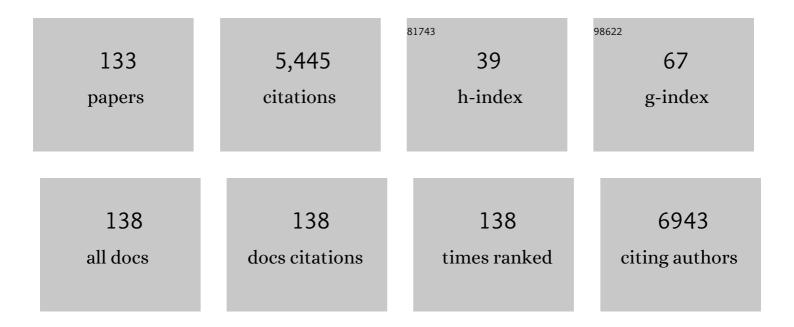
Jaco J M Zwanenburg

List of Publications by Year in descending order

Source: https://exaly.com/author-pdf/4446134/publications.pdf Version: 2024-02-01



#	Article	IF	CITATIONS
1	Interventricular Mechanical Asynchrony in Pulmonary Arterial Hypertension. Journal of the American College of Cardiology, 2008, 51, 750-757.	1.2	364
2	Clinical applications of 7T MRI in the brain. European Journal of Radiology, 2013, 82, 708-718.	1.2	219
3	Myocardial Strain and Torsion Quantified by Cardiovascular Magnetic Resonance Tissue Tagging. Journal of the American College of Cardiology, 2006, 48, 2002-2011.	1.2	189
4	<i>In Vivo</i> Detection of Cerebral Cortical Microinfarcts with High-Resolution 7T MRI. Journal of Cerebral Blood Flow and Metabolism, 2013, 33, 322-329.	2.4	177
5	Subfields of the hippocampal formation at 7T MRI: In vivo volumetric assessment. NeuroImage, 2012, 61, 1043-1049.	2.1	160
6	The Use and Pitfalls of Intracranial Vessel Wall Imaging: How We Do It. Radiology, 2018, 286, 12-28.	3.6	152
7	Imaging Intracranial Vessel Wall Pathology With Magnetic Resonance Imaging. Circulation, 2014, 130, 192-201.	1.6	143
8	Increased cortical grey matter lesion detection in multiple sclerosis with 7 T MRI: a post-mortem verification study. Brain, 2016, 139, 1472-1481.	3.7	133
9	Intracranial Vessel Wall Imaging at 7.0-T MRI. Stroke, 2011, 42, 2478-2484.	1.0	123
10	Timing of cardiac contraction in humans mapped by high-temporal-resolution MRI tagging: early onset and late peak of shortening in lateral wall. American Journal of Physiology - Heart and Circulatory Physiology, 2004, 286, H1872-H1880.	1.5	104
11	Visualization of Perivascular Spaces and Perforating Arteries With 7 T Magnetic Resonance Imaging. Investigative Radiology, 2014, 49, 307-313.	3.5	102
12	Highâ€resolution magnetizationâ€prepared 3Dâ€FLAIR imaging at 7.0 Tesla. Magnetic Resonance in Medicine, 2010, 64, 194-202.	1.9	101
13	Assessment of blood flow velocity and pulsatility in cerebral perforating arteries with 7â€T quantitative flow MRI. NMR in Biomedicine, 2016, 29, 1295-1304.	1.6	91
14	Correction of phase offset errors in main pulmonary artery flow quantification. Journal of Magnetic Resonance Imaging, 2005, 22, 73-79.	1.9	89
15	Cerebral Microbleeds on MR Imaging: Comparison between 1.5 and 7T. American Journal of Neuroradiology, 2011, 32, 1043-1049.	1.2	85
16	Steady-state free precession with myocardial tagging: CSPAMM in a single breathhold. Magnetic Resonance in Medicine, 2003, 49, 722-730.	1.9	79
17	High Prevalence of Cerebral Microbleeds at 7Tesla MRI in Patients with Early Alzheimer's Disease. Journal of Alzheimer's Disease, 2012, 31, 259-263.	1.2	78
18	Cerebral amyloid angiopathy severity is linked to dilation of juxtacortical perivascular spaces. Journal of Cerebral Blood Flow and Metabolism, 2016, 36, 576-580.	2.4	76

#	Article	IF	CITATIONS
19	Lesion detection at seven Tesla in multiple sclerosis using magnetisation prepared 3D-FLAIR and 3D-DIR. European Radiology, 2012, 22, 221-231.	2.3	73
20	Imaging the Intracranial Atherosclerotic Vessel Wall Using 7T MRI: Initial Comparison with Histopathology. American Journal of Neuroradiology, 2015, 36, 694-701.	1.2	70
21	Automated Hippocampal Subfield Segmentation at 7T MRI. American Journal of Neuroradiology, 2016, 37, 1050-1057.	1.2	66
22	Lines of Baillarger in vivo and ex vivo: Myelin contrast across lamina at 7 T MRI and histology. NeuroImage, 2016, 133, 163-175.	2.1	66
23	MR angiography of the cerebral perforating arteries with magnetization prepared anatomical reference at 7T: Comparison with timeâ€ofâ€flight. Journal of Magnetic Resonance Imaging, 2008, 28, 1519-1526.	1.9	65
24	Higher Pulsatility in Cerebral Perforating Arteries in Patients With Small Vessel Disease Related Stroke, a 7T MRI Study. Stroke, 2019, 50, 62-68.	1.0	65
25	Clinical application of multi-contrast 7-T MR imaging in multiple sclerosis: increased lesion detection compared to 3ÂT confined to grey matter. European Radiology, 2013, 23, 528-540.	2.3	64
26	Fast high resolution whole brain T2* weighted imaging using echo planar imaging at 7T. NeuroImage, 2011, 56, 1902-1907.	2.1	59
27	Multi-sequence whole-brain intracranial vessel wall imaging at 7.0 tesla. European Radiology, 2013, 23, 2996-3004.	2.3	59
28	High-resolution intracranial vessel wall MRI in an elderly asymptomatic population: comparison of 3T and 7T. European Radiology, 2017, 27, 1585-1595.	2.3	59
29	Fluid attenuated inversion recovery (FLAIR) MRI at 7.0 Tesla: comparison with 1.5 and 3.0ÂTesla. European Radiology, 2010, 20, 915-922.	2.3	58
30	Quantification and visualization of flow in the Circle of Willis: Timeâ€resolved threeâ€dimensional phase contrast MRI at 7 T compared with 3 T. Magnetic Resonance in Medicine, 2013, 69, 868-876.	1.9	58
31	Multicontrast MR Imaging at 7T in Multiple Sclerosis: Highest Lesion Detection in Cortical Gray Matter with 3D-FLAIR. American Journal of Neuroradiology, 2013, 34, 791-796.	1.2	57
32	Visualization of the Aneurysm Wall. Neurosurgery, 2014, 75, 614-622.	0.6	55
33	The Spectrum of MR Detectable Cortical Microinfarcts: A Classification Study with 7-Tesla Postmortem MRI and Histopathology. Journal of Cerebral Blood Flow and Metabolism, 2015, 35, 676-683.	2.4	54
34	Noninvasive Depiction of the Lenticulostriate Arteries with Time-of-Flight MR Angiography at 7.0 T. Cerebrovascular Diseases, 2008, 26, 624-629.	0.8	52
35	Targeting Cerebral Small Vessel Disease With MRI. Stroke, 2017, 48, 3175-3182.	1.0	52
36	Propagation of Onset and PeakTime of Myocardial Shortening in Time of Myocardial Shortening in Ischemic Versus Nonischemic Cardiomyopathy. Journal of the American College of Cardiology, 2005, 46, 2215-2222.	1.2	51

#	Article	IF	CITATIONS
37	Does Myocardial Fibrosis Hinder Contractile Function and Perfusion in Idiopathic Dilated Cardiomyopathy? PET and MR Imaging Study. Radiology, 2006, 240, 380-388.	3.6	51
38	Perivascular spaces in MS patients at 7 Tesla MRI: A marker of neurodegeneration?. Multiple Sclerosis Journal, 2015, 21, 155-162.	1.4	50
39	Phase contrast MRI measurements of net cerebrospinal fluid flow through the cerebral aqueduct are confounded by respiration. Journal of Magnetic Resonance Imaging, 2019, 49, 433-444.	1.9	48
40	Perforating arteries originating from the posterior communicating artery: a 7.0-Tesla MRI study. European Radiology, 2009, 19, 2986-2992.	2.3	40
41	Visualization of cerebral microbleeds with dualâ€echo T2*â€weighted magnetic resonance imaging at 7.0 T. Journal of Magnetic Resonance Imaging, 2010, 32, 52-59.	1.9	40
42	Thinner Regions of Intracranial Aneurysm Wall Correlate with Regions of Higher Wall Shear Stress: A 7T MRI Study. American Journal of Neuroradiology, 2016, 37, 1310-1317.	1.2	40
43	Direct detection of myocardial fibrosis by MRI. Journal of Molecular and Cellular Cardiology, 2011, 51, 974-979.	0.9	39
44	Major depressive episodes over the course of 7 years and hippocampal subfield volumes at 7 tesla MRI: The PREDICT-MR study. Journal of Affective Disorders, 2015, 175, 1-7.	2.0	39
45	White matter hyperintensity shape and location feature analysis on brain MRI; proof of principle study in patients with diabetes. Scientific Reports, 2018, 8, 1893.	1.6	39
46	Perivascular spaces on 7 Tesla brain MRI are related to markers of small vessel disease but not to age or cardiovascular risk factors. Journal of Cerebral Blood Flow and Metabolism, 2016, 36, 1708-1717.	2.4	38
47	Abnormalities of Cerebral Deep Medullary Veins on 7 Tesla MRI in Amnestic Mild Cognitive Impairment and Early Alzheimer's Disease: A Pilot Study. Journal of Alzheimer's Disease, 2017, 57, 705-710.	1.2	38
48	Clinical vascular imaging in the brain at 7 T. NeuroImage, 2018, 168, 452-458.	2.1	38
49	Cardiac and respiration-induced brain deformations in humans quantified with high-field MRI. NeuroImage, 2020, 210, 116581.	2.1	38
50	Hippocampal Disconnection in Early Alzheimer's Disease: A 7 Tesla MRI Study. Journal of Alzheimer's Disease, 2015, 45, 1247-1256.	1.2	37
51	High-Resolution Postcontrast Time-of-Flight MR Angiography of Intracranial Perforators at 7.0 Tesla. PLoS ONE, 2015, 10, e0121051.	1.1	37
52	Regional heterogeneity of resting perfusion in hypertrophic cardiomyopathy is related to delayed contrast enhancement but not to systolic function: A PET and MRI study. Journal of Nuclear Cardiology, 2006, 13, 660-667.	1.4	35
53	Extended harmonic phase tracking of myocardial motion: Improved coverage of myocardium and its effect on strain results. Journal of Magnetic Resonance Imaging, 2006, 23, 682-690.	1.9	35
54	Dissected Sentinel Lymph Nodes of Breast Cancer Patients: Characterization with High-Spatial-Resolution 7-T MR Imaging. Radiology, 2011, 261, 127-135.	3.6	35

#	Article	IF	CITATIONS
55	DENSE and HARP: Two views on the same technique of phase-based strain imaging. Journal of Magnetic Resonance Imaging, 2006, 24, 1432-1438.	1.9	34
56	Quantitative Intracranial Atherosclerotic Plaque Characterization at 7T MRI: An Ex Vivo Study with Histologic Validation. American Journal of Neuroradiology, 2016, 37, 802-810.	1.2	34
57	Better and faster velocity pulsatility assessment in cerebral white matter perforating arteries with 7T quantitative flow MRI through improved slice profile, acquisition scheme, and postprocessing. Magnetic Resonance in Medicine, 2018, 79, 1473-1482.	1.9	34
58	T 2 mapping of cerebrospinal fluid: 3ÂT versus 7ÂT. Magnetic Resonance Materials in Physics, Biology, and Medicine, 2018, 31, 415-424.	1.1	33
59	An anomaly detection approach to identify chronic brain infarcts on MRI. Scientific Reports, 2021, 11, 7714.	1.6	33
60	Endogenous assessment of chronic myocardial infarction with T1ϕmapping in patients. Journal of Cardiovascular Magnetic Resonance, 2014, 16, 104.	1.6	32
61	Highâ€resolution MRI of the carotid arteries using a leaky waveguide transmitter and a highâ€density receive array at 7 T. Magnetic Resonance in Medicine, 2013, 69, 1186-1193.	1.9	31
62	Endogenous contrast MRI of cardiac fibrosis: Beyond late gadolinium enhancement. Journal of Magnetic Resonance Imaging, 2015, 41, 1181-1189.	1.9	30
63	7 tesla T2*-weighted MRI as a tool to improve detection of focal cortical dysplasia. Epileptic Disorders, 2016, 18, 315-323.	0.7	30
64	Endogenous assessment of diffuse myocardial fibrosis in patients with T _{1Ï} -mapping. Journal of Magnetic Resonance Imaging, 2017, 45, 132-138.	1.9	30
65	Mechanical dyssynchrony or myocardial shortening as MRI predictor of response to biventricular pacing?. Journal of Magnetic Resonance Imaging, 2007, 26, 1452-1460.	1.9	29
66	Quantifying cardiacâ€induced brain tissue expansion using DENSE. NMR in Biomedicine, 2019, 32, e4050.	1.6	28
67	Regional timing of myocardial shortening is related to prestretch from atrial contraction: assessment by high temporal resolution MRI tagging in humans. American Journal of Physiology - Heart and Circulatory Physiology, 2005, 288, H787-H794.	1.5	27
68	Quantification of deep medullary veins at 7 T brain MRI. European Radiology, 2016, 26, 3412-3418.	2.3	27
69	ExÂvivo vessel wall thickness measurements of the human circle of Willis using 7T MRI. Atherosclerosis, 2018, 273, 106-114.	0.4	27
70	MRI of the carotid artery at 7 Tesla: Quantitative comparison with 3 Tesla. Journal of Magnetic Resonance Imaging, 2015, 41, 773-780.	1.9	26
71	The effect of left bundle branch block on left ventricular remodeling, dyssynchrony and deformation of the mitral valve apparatus: an observational cardiovascular magnetic resonance imaging study. International Journal of Cardiovascular Imaging, 2007, 23, 529-536.	0.7	25
72	Characterization of ex vivo healthy human axillary lymph nodes with high resolution 7 Tesla MRI. European Radiology, 2011, 21, 310-317.	2.3	23

#	Article	IF	CITATIONS
73	Microbleeds colocalize with enlarged juxtacortical perivascular spaces in amnestic mild cognitive impairment and early Alzheimer's disease: A 7 Tesla MRI study. Journal of Cerebral Blood Flow and Metabolism, 2020, 40, 739-746.	2.4	23
74	Generalized Multiple-Layer Appearance of the Cerebral Cortex with 3D FLAIR 7.0-T MR Imaging. Radiology, 2012, 262, 995-1001.	3.6	22
75	Distribution and natural course of intracranial vessel wall lesions in patients with ischemic stroke or TIA at 7.0 tesla MRI. European Radiology, 2015, 25, 1692-1700.	2.3	22
76	7-T MRI in Cerebrovascular Diseases. Topics in Magnetic Resonance Imaging, 2016, 25, 89-100.	0.7	21
77	Validating faster DENSE measurements of cardiac-induced brain tissue expansion as a potential tool for investigating cerebral microvascular pulsations. NeuroImage, 2020, 208, 116466.	2.1	21
78	Vasodilatory Capacity of the Cerebral Vasculature in Patients with Carotid Artery Stenosis. American Journal of Neuroradiology, 2011, 32, 1030-1033.	1.2	20
79	Cerebral Lesions on 7 Tesla MRI in Patients with Sickle Cell Anemia. Cerebrovascular Diseases, 2015, 39, 181-189.	0.8	20
80	Detecting Intracranial Vessel Wall Lesions With 7T-Magnetic Resonance Imaging. Stroke, 2017, 48, 2601-2604.	1.0	20
81	Assessment of Myocardial Fibrosis in Mice Using a T2*-Weighted 3D Radial Magnetic Resonance Imaging Sequence. PLoS ONE, 2015, 10, e0129899.	1.1	19
82	FID sampling superior to spinâ€echo sampling for <i>T</i> â€based quantification of holmiumâ€loaded microspheres: Theory and experiment. Magnetic Resonance in Medicine, 2008, 60, 1466-1476.	1.9	18
83	7.0 T MRI Detection of Cerebral Microinfarcts in Patients with a Symptomatic High-Grade Carotid artery Stenosis. Journal of Cerebral Blood Flow and Metabolism, 2014, 34, 1715-1719.	2.4	18
84	Detailed view on slow sinusoidal, hemodynamic oscillations on the human brain cortex by <scp>F</scp> ourier transforming oxy/deoxy hyperspectral images. Human Brain Mapping, 2018, 39, 3558-3573.	1.9	18
85	Single Breath-Hold T1ϕMapping of the Heart for Endogenous Assessment of Myocardial Fibrosis. Investigative Radiology, 2016, 51, 505-512.	3.5	17
86	Hypertensive cerebral hemorrhage. Neurology, 2010, 75, 572-573.	1.5	16
87	Adiabatic turbo spin echo in human applications at 7 T. Magnetic Resonance in Medicine, 2012, 68, 580-587.	1.9	16
88	Assessing Cortical Cerebral Microinfarcts on High Resolution MR Images. Journal of Visualized Experiments, 2015, , .	0.2	16
89	Inter-patient variations in flow boundary conditions at middle cerebral artery from 7T PC-MRI and influence on Computational Fluid Dynamics of intracranial aneurysms. Computers in Biology and Medicine, 2020, 120, 103759.	3.9	16
90	Data on vessel wall thickness measurements of intracranial arteries derived from human circle of Willis specimens. Data in Brief, 2018, 19, 6-12.	0.5	15

#	Article	IF	CITATIONS
91	Cerebrospinal fluid volumetric MRI mapping as a simple measurement for evaluating brain atrophy. European Radiology, 2016, 26, 1254-1262.	2.3	14
92	Velocity Pulsatility and Arterial Distensibility Along the Internal Carotid Artery. Journal of the American Heart Association, 2020, 9, e016883.	1.6	14
93	Nonâ€Invasive Assessment of Damping of Blood Flow Velocity Pulsatility in Cerebral Arteries With <scp>MRI</scp> . Journal of Magnetic Resonance Imaging, 2022, 55, 1785-1794.	1.9	14
94	Ischaemic Cavities in the Cerebellum: An ex vivo 7-Tesla MRI Study with Pathological Correlation. Cerebrovascular Diseases, 2014, 38, 17-23.	0.8	13
95	Seven-Tesla Magnetic Resonance Imaging of Atherosclerotic Plaque in the Significantly Stenosed Carotid Artery. Investigative Radiology, 2014, 49, 749-757.	3.5	13
96	FLAIR images at 7 Tesla MRI highlight the ependyma and the outer layers of the cerebral cortex. NeuroImage, 2015, 104, 100-109.	2.1	13
97	Quantitative T1 mapping under precisely controlled graded hyperoxia at 7T. Journal of Cerebral Blood Flow and Metabolism, 2017, 37, 1461-1469.	2.4	13
98	Vascular reactivity in small cerebral perforating arteries with 7†T phase contrast MRI – A proof of concept study. NeuroImage, 2018, 172, 470-477.	2.1	13
99	Automated Assessment of Cerebral Arterial Perforator Function on 7T MRI. Journal of Magnetic Resonance Imaging, 2021, 53, 234-241.	1.9	13
100	Comparison of 3T Intracranial Vessel Wall MRI Sequences. American Journal of Neuroradiology, 2018, 39, 1112-1120.	1.2	12
101	Qualitative Evaluation of a High-Resolution 3D Multi-Sequence Intracranial Vessel Wall Protocol at 3 Tesla MRI. PLoS ONE, 2016, 11, e0160781.	1.1	12
102	Quantitative comparison of 2D and 3D circumferential strain using MRI tagging in normal and LBBB hearts. Magnetic Resonance in Medicine, 2007, 57, 485-493.	1.9	11
103	Relations between location and type of intracranial atherosclerosis and parenchymal damage. Journal of Cerebral Blood Flow and Metabolism, 2016, 36, 1271-1280.	2.4	11
104	Automated Multi-Atlas Segmentation of Hippocampal and Extrahippocampal Subregions in Alzheimer's Disease at 3T and 7T: What Atlas Composition Works Best?. Journal of Alzheimer's Disease, 2018, 63, 217-225.	1.2	11
105	Branching Pattern of the Cerebral Arterial Tree. Anatomical Record, 2019, 302, 1434-1446.	0.8	11
106	Does the Internal Carotid Artery Attenuate Bloodâ€Flow Pulsatility in Small Vessel Disease? A 7ÂT <scp>4D</scp> â€Flow <scp>MRI</scp> Study. Journal of Magnetic Resonance Imaging, 2022, 56, 527-535.	1.9	10
107	Myelin contrast across lamina at 7T, ex-vivo and in-vivo dataset. Data in Brief, 2016, 8, 990-1003.	0.5	9
108	Quantification of Intracranial Aneurysm Volume Pulsation with 7T MRI. American Journal of Neuroradiology, 2018, 39, 713-719.	1.2	8

#	Article	IF	CITATIONS
109	Intracranial Vessel Wall Magnetic Resonance Imaging Does Not Allow for Accurate and Precise Wall Thickness Measurements. Stroke, 2019, 50, e283-e284.	1.0	8
110	Zooming in on cerebral small vessel function in small vessel diseases with 7T MRI: Rationale and design of the "ZOOM@SVDs―study. Cerebral Circulation - Cognition and Behavior, 2021, 2, 100013.	0.4	8
111	Subvoxel vessel wall thickness measurements of the intracranial arteries using a convolutional neural network. Medical Image Analysis, 2021, 67, 101818.	7.0	7
112	Strain Tensor Imaging: Cardiac-induced brain tissue deformation in humans quantified with high-field MRI. NeuroImage, 2021, 236, 118078.	2.1	7
113	High Resolution Imaging of Cerebral Small Vessel Disease with 7 T MRI. Acta Neurochirurgica Supplementum, 2014, 119, 125-130.	0.5	6
114	Pulsatility Index in the Basal Ganglia Arteries Increases with Age in Elderly with and without Cerebral Small Vessel Disease. American Journal of Neuroradiology, 2022, 43, 540-546.	1.2	6
115	Dynamic brain <scp>ADC</scp> variations over the cardiac cycle andÂtheir relation to tissue strain assessed with <scp>DENSE</scp> atÂhighâ€field <scp>MRI</scp> . Magnetic Resonance in Medicine, 2022, 88, 266-279.	1.9	6
116	Automatic quantification of perivascular spaces in T2-weighted images at 7 T MRI. Cerebral Circulation - Cognition and Behavior, 2022, 3, 100142.	0.4	6
117	Histopathology of Cerebral Microinfarcts and Microbleeds in Spontaneous Intracerebral Hemorrhage. Translational Stroke Research, 2023, 14, 174-184.	2.3	6
118	Ultra-High-Field MR Imaging. PET Clinics, 2013, 8, 311-328.	1.5	5
119	High resolution 7T and 9.4T-MRI of human cerebral arterial casts enables accurate estimations of the cerebrovascular morphometry. Scientific Reports, 2018, 8, 14235.	1.6	5
120	Arterial Remodeling of the Intracranial Arteries in Patients With Hypertension and Controls. Hypertension, 2021, 77, 135-146.	1.3	5
121	Detecting low blood concentrations in joints using T1 and T2 mapping at 1.5, 3, and 7 T: an in vitro study. European Radiology Experimental, 2021, 5, 51.	1.7	5
122	Double delay alternating with nutation for tailored excitation facilitates bandingâ€free isotropic highâ€resolution intracranial vessel wall imaging. NMR in Biomedicine, 2021, 34, e4567.	1.6	3
123	Single shot MR tagging to quantify local tissue deformation during MRI-guided needle interventions: A feasibility study. Medical Physics, 2011, 38, 5321-5329.	1.6	2
124	Automated detection of periventricular veins on 7 T brain MRI. Proceedings of SPIE, 2015, , .	0.8	2
125	Blood Flow Velocity Pulsatility and Arterial Diameter Pulsatility Measurements of the Intracranial Arteries Using 4D PC-MRI. Neuroinformatics, 2022, 20, 317-326.	1.5	2
126	Cerebral Small Vessel Disease In Patients With Sickle Cell Disease: Initial Findings With Ultra-High Field 7T MRI. Blood, 2013, 122, 1011-1011.	0.6	2

#	Article	IF	CITATIONS
127	Perforating artery flow velocity and pulsatility in patients with carotid occlusive disease. A 7 tesla MRI study. Cerebral Circulation - Cognition and Behavior, 2022, 3, 100143.	0.4	2
128	Pulsatility Attenuation along the Carotid Siphon in Pseudoxanthoma Elasticum. American Journal of Neuroradiology, 2021, 42, 2030-2033.	1.2	1
129	Advances in MRI for Elective Treatment of Lymph Nodes and Cranial Nerves in Head and Neck Cancer. International Journal of Radiation Oncology Biology Physics, 2014, 90, S570-S571.	0.4	Ο
130	Cover Image, Volume 29, Issue 9. NMR in Biomedicine, 2016, 29, i-i.	1.6	0
131	Increased Rather than Decreased Small Vessel Pulsatility in Patients with Progressing Cerebral White Matter Hyperintensities. Radiology, 2018, 286, 363-364.	3.6	Ο
132	Diagnostic Ability of CT to Help Differentiate Stenosis of 30% in Patients with Atrial Fibrillation. Radiology, 2018, 286, 361-363.	3.6	0
133	Subvoxel vessel wall thickness measurements from vessel wall MR images. , 2019, , .		Ο